

# AMR-MHD Simulation of CME Propagation in Solar Wind Generated on Split Dodecahedron Grid

Tomoya Ogawa<sup>1</sup>, Mitsue Den<sup>2</sup>, Takashi Tanaka<sup>2,3</sup> and  
Kazuyuki Yamashita<sup>4</sup>

<sup>1</sup>Kitasato University, 1-15-1 Kitasato, Minami-ku, Sagami-hara, Kanagawa 252-0373, Japan  
email: [ogawa@kitasato-u.ac.jp](mailto:ogawa@kitasato-u.ac.jp)

<sup>2</sup>National Institute of Information and Communications Technology, Koganei, Tokyo, Japan

<sup>3</sup>Kyushu University, Fukuoka, Japan

<sup>4</sup>University of Yamanashi, Kofu, Yamanashi, Japan

**Abstract.** We perform simulations of the interplanetary coronal mass ejections relating to the magnetic storm on 17 March 2015. A hierarchical mesh structure is used, which is controlled by an adaptive mesh refinement technique, with fine-scale cells where it matters, the structure of the running shock waves of the coronal mass ejections and co-rotating interactive regions. The initial and the inner-boundary conditions are derived from another simulation, which uses a split dodecahedron grid. The resulting shock-wave with the models adjusted to the observed ejection speed on the sky plane show delays by 20% in the arrival time at the Earth from the observed data. By contrast, the model adjusted to the observed arrival time at the Earth needs the ejection speed 30% higher than that in the above models.

**Keywords.** MHD, methods: numerical, Sun: coronal mass ejections (CMEs), solar wind

---

## 1. Introduction

A coronal mass ejection (CME) occurred on 15 Mar 2015, accompanied by an X-ray flare at S22W25. A shock wave generated by the CME, which subsequently reached the Earth, was unexpectedly strong and triggered a geomagnetic storm on 17 Mar 2015. In such a case, the interaction with the background solar-wind structure is considered to play an important role in the propagation of CME-caused shock waves. We have developed a magnetohydrodynamics (MHD) code, in which a hierarchical Cartesian mesh was used and an adaptive mesh refinement (AMR) technique was employed. The AMR technique enables us to trace running structures, e.g. CME-caused shock waves and co-rotating interaction regions (CIRs), with fine-scale cells. Simulations of propagation of interplanetary shock waves are performed and their results are compared with the observed data.

## 2. Method

First, the background solar wind structure should be determined. For the purpose, we employ an MHD code that uses a split dodecahedron grid, which is spherical and has no polar singularity (Nakamizo *et al.* 2009 and Den *et al.* 2015). We use the photospheric magnetic field data obtained by the Global Oscillation Network Group (GONG) and calculate the steady-state solar wind with the method by Den *et al.* (2015). The derived

parameters of the solar wind are input to the AMR-MHD simulations as the initial and the inner-boundary conditions.

Second, we introduce the CME models. We focus on two CMEs: the halo CME on 15 March 2015, which triggered the geomagnetic storm, and the preceding partial halo CME on 14 March. The latter was very weak, but it may have affected the shock wave propagation, given that the subsequent CME seems to have caught up with it.

We model a CME as the cone velocity,  $V_r(t, \xi) = T(t) \cdot V_0 \cos(\xi/2)$ , where  $\xi$  is an angle from the cone axis,  $T(t)$  is a trapezoidal pulse characterized by the three parameters of duration times of rising  $d_1$ , maintaining maximum  $d_2$ , and decline  $d_3$ , and where  $V_0$  is the maximum velocity on the cone axis (Odstrcil & Pizzo 1999). The values of  $d_1$ ,  $d_2$ ,  $d_3$ , and  $V_0$  are determined from the observed values, i.e. the durations of relating X-ray flares and the CME speeds on the sky plane in the SOHO/LASCO CME Catalog; they are  $d_1 = 85\text{min}$ ,  $d_2 = 85\text{min}$ ,  $d_3 = 240\text{min}$ , and  $V_0 = 1068\text{km/s}$  for the halo CME, and  $d_1 = 20\text{min}$ ,  $d_2 = 10\text{min}$ ,  $d_3 = 210\text{min}$ , and  $V_0 = 564\text{km/s}$  for the partial-halo CME. We introduce three models: background solar-wind only (model 1), the halo CME input (model 2), and the two CMEs input (model 3). In addition, we use an extra model (model 4), in which the two CMEs with the same parameter values as in model 3 but  $V_0 = 1388\text{km/s}$  for the halo CME to adjust to the arrival time of the shock wave observed by the ACE space craft.

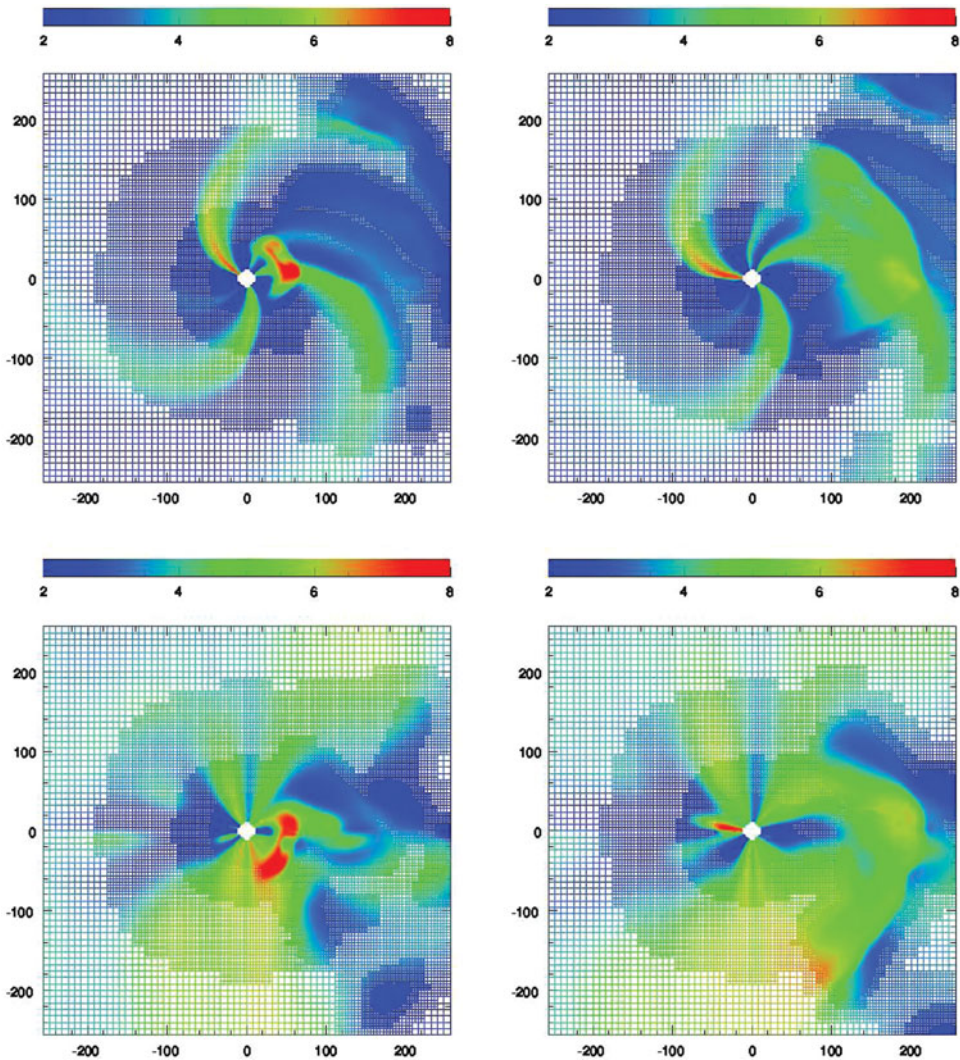
### 3. Results

Figure 1 shows our simulation results of the velocity distributions and mesh structures with model 3. The cells with the finest size of  $1R_s$  successfully catch the running shock wave and CIRs. Note that we have made mesh refinement for the region only within the longitude of  $\pm 60\text{deg}$  and latitude of  $\pm 60\text{deg}$  and set the cell size finest near the sun.

Next, we compare the time profiles of velocity and density of 4 models with one another and the observed data by the ACE space craft (Figure 2). Several small gaps are identified in the profiles, which correspond to the points where the cell size changes. The results with models 2 and 3 show marginal differences only. It implies that the effect of the preceding partial halo CME is small. The shock waves with models 2 and 3 are found to be weaker and arrive later than the observed. By contrast, the peaks of velocity and density with model 4 show good agreement with the observation.

### 4. Discussion and conclusions

The steady-state solar wind derived on a split dodecahedron grid is input to the AMR-MHD simulations and it then generates the background structure. The dynamic mesh captures the CIRs with a high resolution. A running shock wave is also successfully captured with a high resolution and is found to maintain its sharp shape even at the arrival at the Earth. The results with models 2 and 3 show only a marginal difference from each other. The arrival times of the shock waves on the ACE's position with models 2 and 3, in which the CME velocities are determined by the observed value in the solar corona, are about 20% later than the observation. By contrast, that and the peaks of the velocity and density with model 4, in which the CME speed is 30% higher than the coronal observation, show good agreement with the ACE's observation. The after-shock velocities with models 2, 3 and 4 are underestimated. These results suggest that there is a margin for improvement in our CME model.



**Figure 1.** Two-dimensional color map of the simulated results of radial component of the velocity (color-bar scale in units of  $81.52\text{km/s}$ ) with model 3 on the (upper panels) equatorial and (lower panels) meridional planes at (left panels) 12 and (right panels) 60 hours after the halo CME occurs. The mesh structures in the simulations are indicated by grids.

## 5. Acknowledgement

This work utilizes the data obtained by the Global Oscillation Network Group (GONG) program, managed by the National Solar Observatory, which is operated by AURA, Inc. under a cooperative agreement with the National Science Foundation. The data were acquired by instruments operated by the Big Bear Solar Observatory, High Altitude Observatory, Learmonth Solar Observatory, Udaipur Solar Observatory, Instituto de Astrofísica de Canarias, and Cerro Tololo Interamerican Observatory.

We use the data from the SOHO/LASCO CME Catalog, which was generated and is maintained at the CDAW Data Center by NASA and The Catholic University of America in cooperation with the Naval Research Laboratory. SOHO is a project of international cooperation between ESA and NASA.

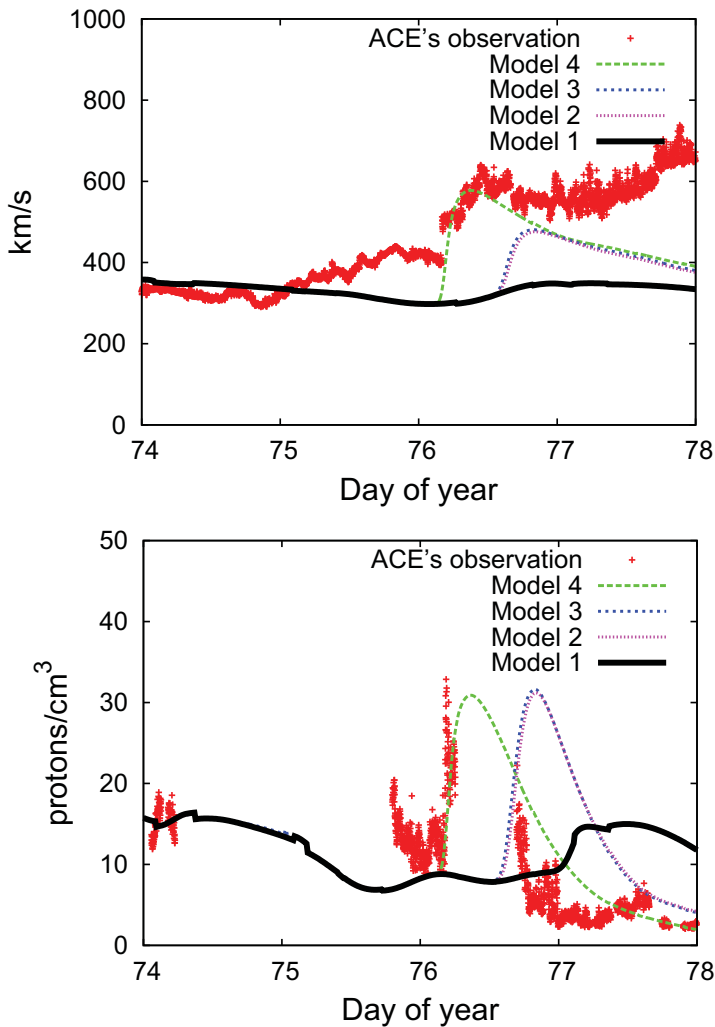


**Figure 2.** (Upper panel) Time profile of velocity in  $km/s$  for the 4 models at the ACE's position, compared with the observation by ACE. The horizontal axis is time in units of day of a year. (Lower panel) Proton number density in  $cm^{-3}$  for the same models.

We thank the ACE SWEPAM instrument team and the ACE Science Center for providing the ACE data.

## References

- Den, M., Tanaka, T., Kubo, Y. & Watari, S. 2015, *34th Int. Cosmic Ray Conf.*, 184  
 Khokhlov, A. M. 1998, *J. Comput. Phys.*, 143, 519  
 Nakamizo, A., Tanaka, T., Kubo, Y., Kamei, S. & Shimazu, H. 2009, *J. Geophys. Res.*, 114, A07109  
 Odstrcil, D. & Pizzo, V. J. 1999, *J. Geophys. Res.*, 104, 483